Supporting Information

Thermal proteome profiling of itaconate interactome in macrophages

Yunzhu Meng,[†a,b] Tiantian Wei,[†a,c,d] Chenlin Zhang,[a,b] Anqi Yu,[a,b] Yuan Liu,[a,b] Junyu Xiao[a,d] and Chu Wang[*a,b,e]

[a.] *Peking-Tsinghua Center for Life Sciences, Academy for Advanced Interdisciplinary Studies, Peking University, Beijing 100871, China.*

[b.] *Synthetic and Functional Biomolecules Center, Beijing National Laboratory for Molecular Sciences, Key Laboratory of Bioorganic Chemistry and Molecular Engineering of Ministry of Education, College of Chemistry and Molecular Engineering, Peking University, Beijing 100871, China.*

[c.] *State Key Laboratory of Natural and Biomimetic Drugs, School of Pharmaceutical Sciences, Peking University, Beijing 100191, China.*

[d.] *The State Key Laboratory of Protein and Plant Gene Research, School of Life Sciences, Peking University, Beijing 100871, China.*

[e.] *Peking University Chengdu Academy for Advanced Interdisciplinary Biotechnologies, Chengdu 610231, China.*

† These authors contributed equally to this work.

Table of Contents

Supplementary Figures

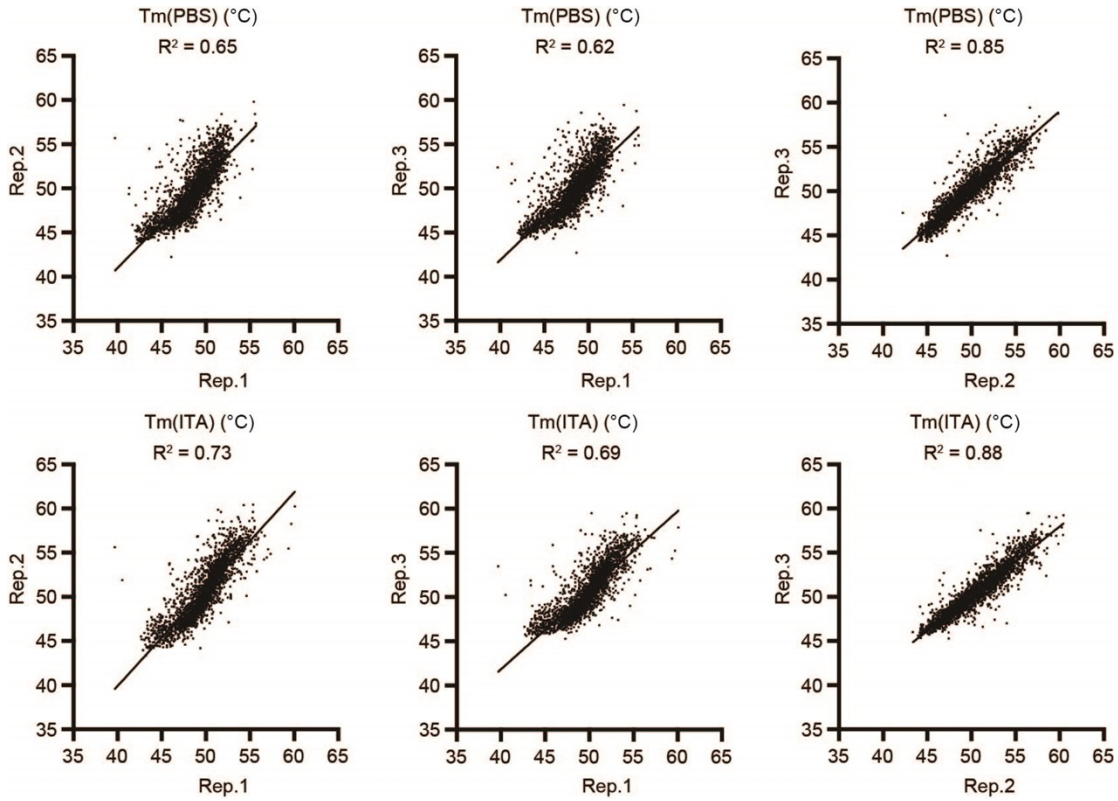

Figure S1. Pearson correlation analysis of T_m values quantified for each protein across three biological replicates.

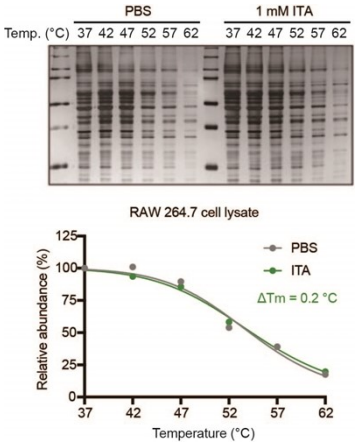

Figure S2. The global thermal stability of cell lysates with ITA treatment.

The global thermal stability of RAW 264.7 lysate was barely changed after ITA treatment as visualized by gel staining.

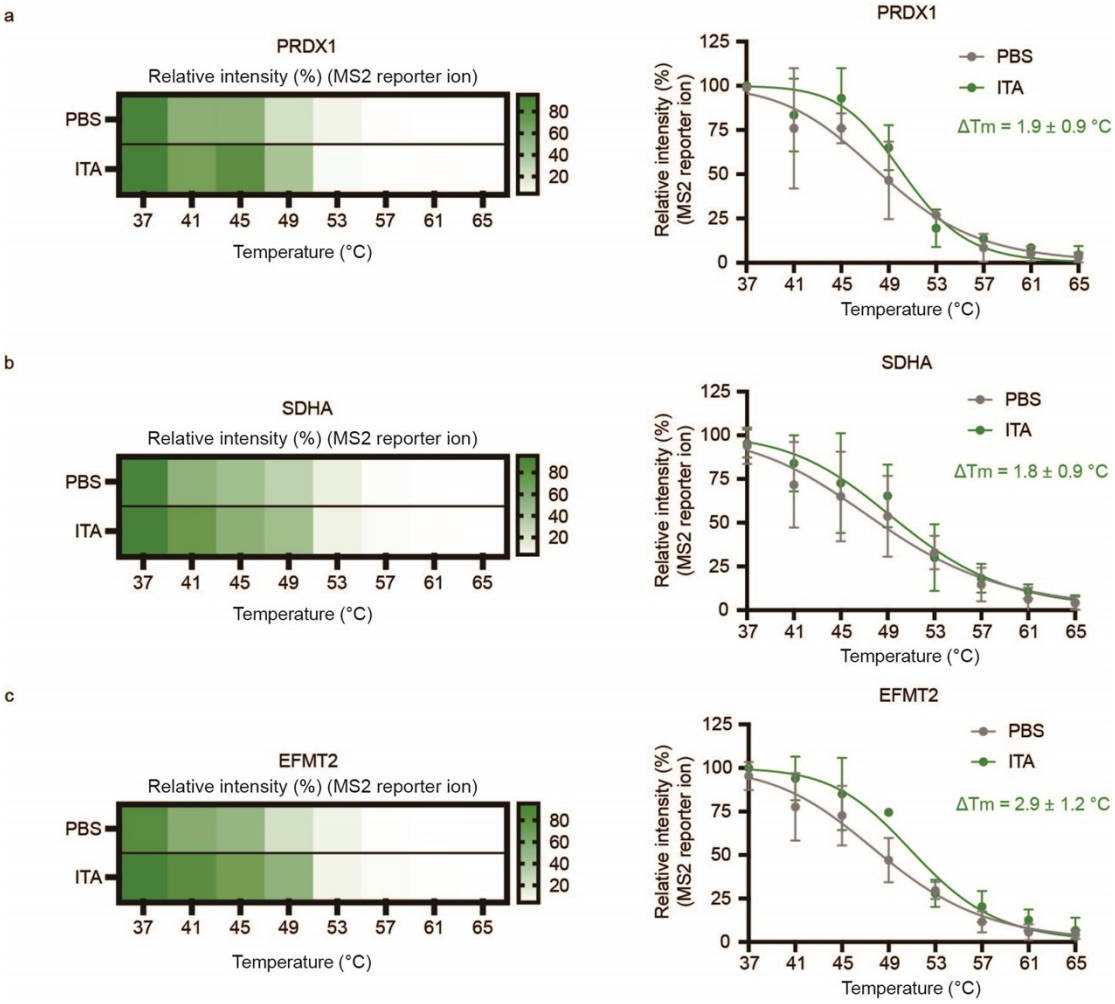

Figure S3. Thermal melting curve of selected ITA targets in MS-based TPP data.

(a-c) Thermal melting curve of PRDX1(**a**), SDHA (**b**), and EFMT2 (**c**), as quantified by MS2 reporter ion intensity from the TPP data.

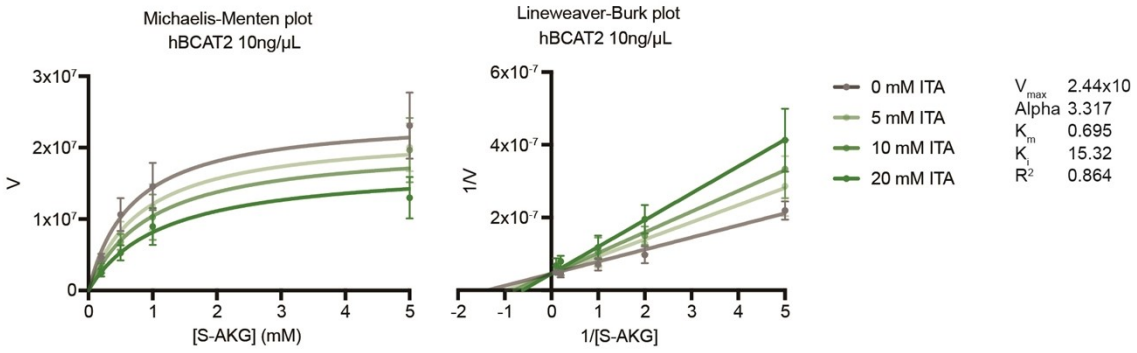

Figure S4. Michaelis-Menten kinetics analysis of BCAT2 activity.

Michaelis-Menten curves and Lineweaver-Burk plot of BCAT2 activity in the presence of increasing itaconate concentrations (0–20 mM) confirmed competitive inhibition.

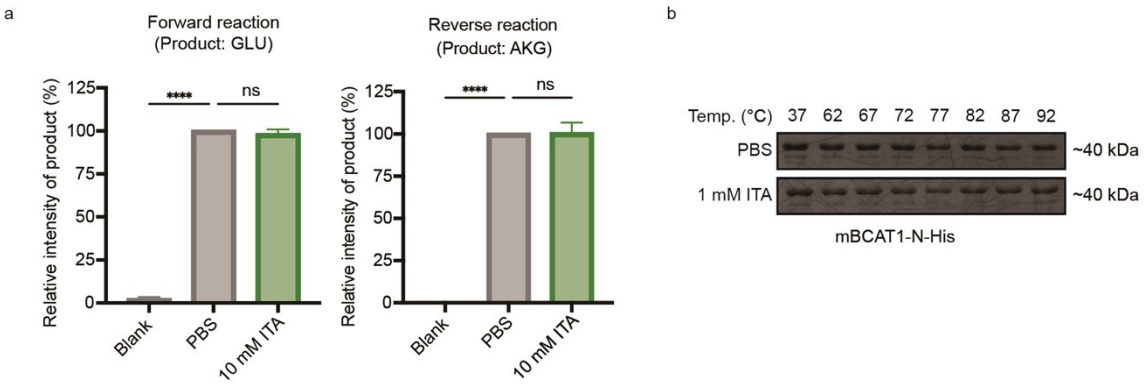

Figure S5. ITA does not interact with BCAT1.

(**a**) ITA hardly inhibited activity of mBCAT1.

(**b**) Thermal stability changes of mBCAT1-N-His caused by ITA.

All results are from three independent experiments. *p < 0.05, **P < 0.01, ***P < 0.001, ****P < 0.0001. Statistical differences were determined by ordinary one-way ANOVA.

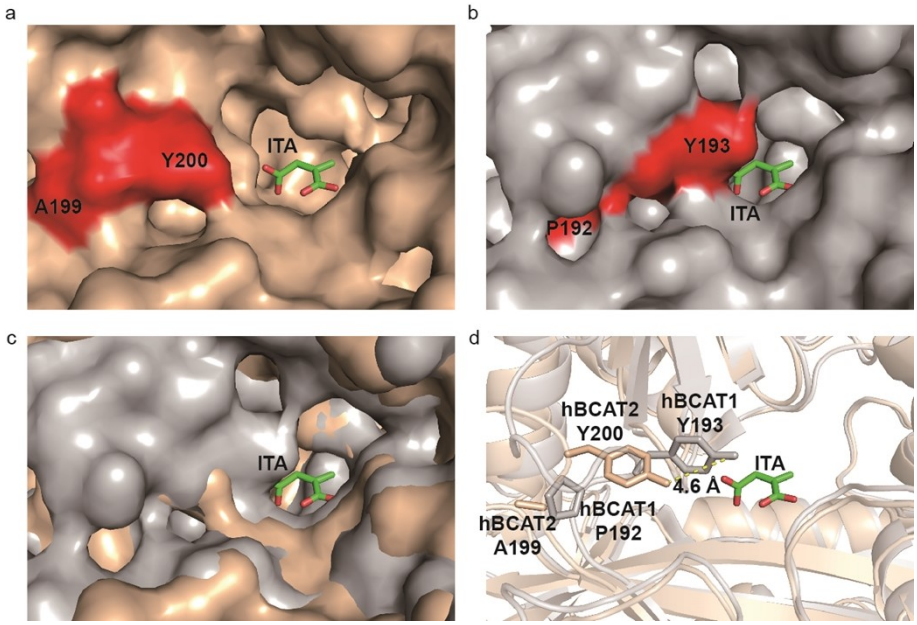

Figure S6. Comparison of ITA docking site between hBCAT2-ITA complex (PDB: 9LEP) and reported inhibitor-bound hBCAT1 structures (PDB: 7NWA).

(a) ITA binding to the hBCAT2 substrate binding site as seen in the co-crystal structure, Ala199-Tyr200 are shown in red color.

(b) ITA modeled into the hBCAT1 substrate binding site as seen in the gray surface structure, Pro192-Tyr193 are shown in red color.

(c) The structural alignments between hBCAT1 and hBCAT2-ITA complex surface models.

(d) The difference between hBCAT1 and hBCAT2-ITA complex stick models, hBCAT2 contains Ala199-Tyr200, which correspond to Pro192-Tyr193 in hBCAT1, The deviation distance between tyrosine residues is indicated by the yellow dotted line.

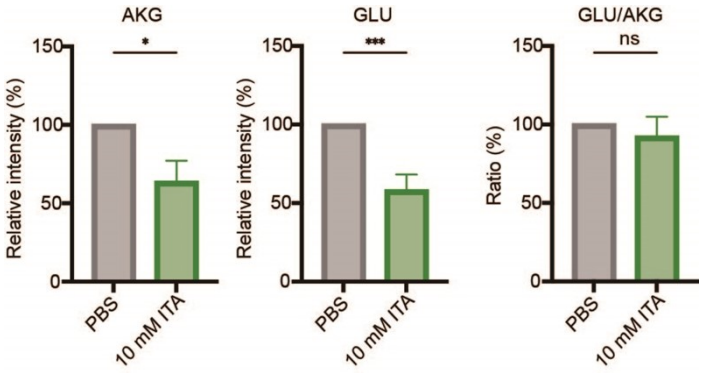

Figure S7. Effects of exogenous ITA on GLU and AKG Level.

Exogenous ITA modulated the relative abundance of GLU and AKG, without significantly affecting their conversion rate.

All results are from three independent experiments. *p < 0.05, **P < 0.01, ***P < 0.001. Statistical differences were determined by ordinary one-way ANOVA.

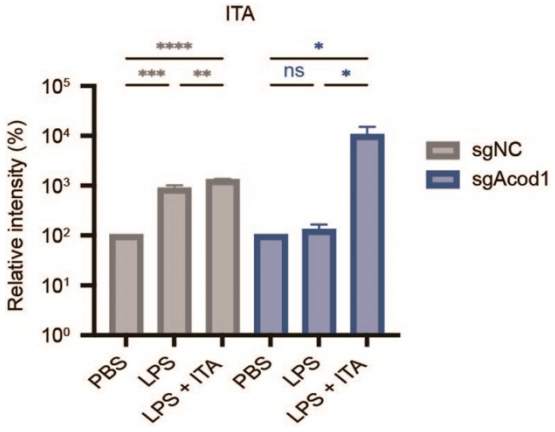

Figure S8. ITA abundance in RAW 264.7 cells after Acod1 knockout.

ITA production was induced by LPS in RAW 246.7 cells. This induction was abolished in the Acod1 knockout cell lines and could be restored by adding exogenous ITA.

All results are from three independent experiments. *p < 0.05, **P < 0.01, ***P < 0.001, ****P < 0.0001. Statistical differences were determined by ordinary one-way ANOVA.

Methods

Cell culture. RAW 264.7 cell line and HEK293T cell line are cultured in DMEM (Thermo Fisher Scientific, Cat# C11995500CP) supplemented with 10% FBS (Gibco, Cat# 10099-141C) and 1% P/S (Gibco, Cat# 15140122) at 37°C in a 5% CO2 incubator.

Plasmids. Full-length complementary DNAs of human and mouse BCAT2, RIPK3 and EFMT2 were obtained from Ensembl Database (BALB/c) and subcloned into pCMV or pCDNA3.1 vector. Mouse BCAT2 and human BCAT2 without mitochondrial transit peptide were also cloned into pQLink-Hx vector.

Antibodies and Reagents. The antibodies used for immunoblotting were: Anti-PRDX1 Rabbit Polyclonal Antibody (lot#00146924, cat. no. 15816-1-AP, Proteintech); Anti-SDHA Rabbit Polyclonal Antibody (lot#00049226, cat. no. 14865-1-AP, Proteintech); Anti-BCAT2 Rabbit Polyclonal Antibody (lot#00089129, cat. no. 16417-1-AP, Proteintech); DDDDK-Tag(binds to flag sequnence) (12M11) Mouse mAb (cat. no. YM3808, Immunoway). Itaconate (cat.no. I29204-100G), LPS (L2630-10MG) were purchased from Sigma. Amino acid and branched-chain keto acid were purchased from Sigma.

TPP assay. RAW 264.7 cells were resuspended in ice-cold PBS and snap-frozen in liquid nitrogen. The tube was placed into a thermal mixer at 25 °C until most of the content was thawed and then transferred to ice until the entire content was thawed. The freeze–thaw cycle was repeated eight times before the samples were subjected to centrifugation (1 hour at 4 °C and 20,000g). The protein concentration of the supernatant was determined using the bicinchoninic acid (BCA) protein assay kit (Pierce). Then, 2 mg/mL lysate (or purified protein diluted by 1x PBS buffer) was incubated with 1 mM ITA or PBS separately for 1 hour at 25 °C, and divided into six or eight aliquots and transferred into 0.2 ml PCR tubes. Each sample was heated in parallel for 3 min to the respective temperature (range from 37-65°C or 37-62°C). Subsequently, the samples were centrifuged at 20,000g for 30 min at 4 °C and the supernatant

was collected. The supernatant was subjected to either gel electrophoresis for gel-based analysis or in-solution digestion, iBT labeling and fractionation for MS-based analysis.

Gel-based analysis. Soluble content was separated using SDS-PAGE. Coomassie Brilliant Blue method and western blot were used to quantify the whole proteome and specific protein in each fraction.

In-solution digestion and iBT labeling. Each sample was adjusted to 6 M urea-PBS buffer for denaturation. Then, 10 mM dithiothreitol (DTT) was added, before incubating at 37 °C for 30 min, followed by the addition of 20 mM iodoacetamide (IAA) for 30 min at 37 °C in the dark. SP3 beads was then used for protein enrichment in 50% ethanol buffer and after washed by 80% ethanol for 3 times, the protein was released into 50 mM ABC buffer. A final concentration of 10 ng/μL of trypsin was added into sample and samples were digested overnight at 37 °C. Then, peptide samples were dried in a SpeedVac, resuspended in 100 mM TEAB (pH 8.5) and labeled with half of iBTpro-16plex reagent (Nanjing Apollomics Biotech Inc. Nanjing, China). The labeling reaction was performed in at 25 °C for 2 h and quenched with 5% hydroxylamine for 15 min. Labeled peptide samples were combined into a new sample for each experiment, and additional fractionation was performed using reversed-phase chromatography at pH 10 by high-performance LC (HPLC).

High-pH reversed-phase HPLC fractionation. To improve protein identification and quantification accuracy, the combined sample was separated into 60 fractions using a high-pH reversed-phase C18 column (Agela Technologies) on the Agilent HPLC system. Mobile phase A consisted of 2% acetonitrile (ACN)–98% H_2O (adjusted to pH 10 with NH3·H2O); mobile phase B consisted of 98% ACN–2% H2O (adjusted to pH 10 with NH3·H2O). Samples were separated using a 60-min gradient of buffer B at a flow rate of 1 ml/min, as follows: 0 min, 0% B; 5 min, 5% B; 15 min, 8% B; 20 min, 16% B; 45 min, 32% B; 45 min, 95% B; 50 min, 95% B; 55 min, 15% B; 60 min, 15% B. The columns were operated at 45 °C and the temperature was controlled using a built-in column heater. The 60 fractions were dried in a SpeedVac and combined into 20 fractions for final LC–MS/MS analysis.

LC-MS/MS analysis. LC–MS/MS analysis was performed on a Q-Exactive Plus mass spectrometer (Thermo Fisher Scientific). The peptides were chromatographically separated by a 60-min gradient from 3% to 60% solvent B (solvent A, 0.1% formic acid in water; solvent B, 0.1% formic acid in 80% ACN) at a flow rate of 300 nL/min. The total measurement time for each sample was 85 min. In positive-ion mode, full-scan mass spectra were acquired over the m/z range from 375 to 1,400 using the Orbitrap mass analyzer with a mass resolution setting of 70,000. MS/MS fragmentation was performed in data-dependent mode, whereby the ten most intense ions were selected from each full-scan mass spectrum for high-energy collision-induced dissociation (HCD) and MS/MS analysis. MS/MS spectra were acquired over the m/z range from 100 to 1,800 with a resolution setting of 35,000 using the Orbitrap analyzer. Other parameters in the centroid format were as follows: isolation window, 1.2 m/z units; default charge, 2+; normalized collision energy, 32%; maximum IT, 100 ms; dynamic exclusion, 20.0 s.

MS data analysis. LC-MS/MS data was analyzed by Proteome Discovery (3.1) with a modified TMT quantification method according to the official parameters of iBTpro-16plex. Full MS and MS/MS spectra were searched against a concatenated forward and reverse version of the mus musculus database downloaded from UniProt (https://www.uniprot.org) with default parameters: a mass tolerance of 20 ppm, the minimum peptide length was seven amino acids. Cysteine modification by IA (carbamidomethyl) was searched as a fixed modification. Methionine oxidation and N-terminal acetylation were searched as variable modifications. The reporter mass tolerance of quantitation labels with 8-plex of iBTpro on the N terminus or lysine was 0.01 Da and trypsin was set as the enzyme with two missed cleavages. The false discovery rate was set at 0.01 for peptides and proteins.

Data normalization and fitting of melting curves. The overall workflow was based on the previously reported method[1]. For iBT quantification, the intensities of the eight reporter ions were collected for each protein and the relative intensity values were calculated using the maximum intensity of the reporter ions corresponding to the two lowest temperatures (37 °C and 41 °C) as the reference on a scale of 0–100%. Then, intensities were corrected for temperature-dependent signal drift using sample-specific correction factors. These corrected

relative intensites were fitted to a sigmoidal curve equation using the curve_fit function from SciPy:

$$f(T) = \frac{100}{1 + \left(\frac{T}{T_m}\right)^{HillSlope}}\%$$

HillSlope represents the sharpness of the melting curve. T_m denotes the temperature at which half of the protein has been denatured: f (T_m) = 50%. The T_m value for each protein was calculated, and only proteins with well-fitted curves ($R^2 \geq 0.8$) were used for further analysis.

Protein purification. Purification method was modified from reported method[2]. Plasmids were transferred into Transetta (DE3) cells. The cells were cultured in traditional LB medium at 37 °C until the optical density (OD) at 600 nm reached between 0.6 and 0.8. The protein overexpression was induced by the addition of isopropyl β-D-1-thiogalactopyranoside (IPTG) to a final concentration of 0.5 mM. After IPTG induction at 18 °C for 20 h, bacterial cells were collected by centrifuging at 4,000 r.p.m. for 30 min and frozen at −80 °C until further use. Bacteria were resuspended in lysis buffer (4 M Urea, 25 mM HEPES, 500 mM NaCl, 0.1 mM PLP, 5 mM β-Me、5% glycerol, 1 mM phenylmethanesulfonylfluoride, pH 7.5) and lysed by sonication. The supernatant was collected after centrifugation at 12,000g for 1 hour and incubated with Ni NTA Beads 6FF (Smart-Lifesciences). Proteins were renatured by using 10 times column volume balance buffer (25 mM HEPES, 500 mM NaCl, 5 mM β-Me、5% glycerol, pH 7.5), and eluted with elution buffer (25 mM HEPES, 500 mM NaCl, 500 mM imidazole, 5 mM β-Me, 5% glycerol, pH 7.5). TEV protease was added for cleaving the His tags at 4 °C for 15 hours. The resulting samples were subjected to a final purification step by size-exclusion chromatography (SEC; Superdex 200 Increase 10/300 GL, GE Healthcare) in storage buffer (25 mM HEPES, 25 mM NaCl, 20 mM DTT, 2.5% glycerol, pH 7.5) or assay buffer (1x PBS, 5 mM β-Me, 5% glycerol, pH 7.5).

Activity assay of the purified BCAT2. 100 mM Stock solution of substrate VAL, KIV, AKG and GLU was configured in 1x PBS buffer at pH 7.4. For forward reaction, 10 mM Val, 5 mM AKG, 5/10 mM ITA, 50 μM PLP, and 0.1 mg/mL BCAT2 were mixed. For reverse reaction, 10

mM KIV, 10 mM GLU, 5/10 mM ITA, 50 μM PLP, and 0.1 mg/mL BCAT2 were mixed. The reaction was performed at 37°C and 300 rpm for 1h, after which 480 μL 0.1%FA was added to terminate the reaction, and after centrifugation, 5 μL was added for LC-MS detection. For Michaelis-Menten kinetics analysis of BCAT2 activity, concentration of BCAT2 were reduced to 0.01 mg/mL and reaction time was reduced to 30 min. Different concentration of AKG (0.2, 0.5, 1,5, 10 mM) and ITA (0, 5, 10, 20 mM) were used.

Quantification of BCAA-related metabolites. RAW 264.7 cells were plated in 6-well plates for one day, and treated with 10 mM ITA or 100 ng/mL LPS for 12 hours, respectively. The cells were washed with PBS gently in the plates for three times and collected by centrifugation. The cells were further washed with PBS for three times by centrifugation. The cell pellets were lysed by sonication in ice-cold 80% methanol to extract the small molecule metabolites, then centrifuged at 20000 g at 4°C for 30 min to remove cell debris. Supernatant was dried in a SpeedVac at 30°C and resuspended by 60 μL 0.1% FA. 5 μL of sample was used for LC-MS detection.

Quantification of small molecules. Intensity of molecules were analyzed by LC-SRM. The LC-SRM system is composed of an AB SCIEX 5500 triple-quadrupole mass spectrometer and a SHIMADZU DGU-20A liquid chromatography instrument with an Agilent column. The buffer gradient is 100%-0 Buffer A (100% water, 0.1% formic acid) and 0%-100% Buffer B (100% methanol, 0.1% formic acid) for 10 min. Metabolites were analyzed according to the following parameters.

	Q1	Q3	DP(eV)	EP(eV)	CE(eV)	CXP(eV)	RT(min)	MOD
GLU	148.1	84.1	93	10	17	10	1.0	+
VAL	118.1	55.2	93	10	13	10	1.5	+
ILE+LEU	132.1	86.0	93	10	13	10	3.15	+
AKG	145.0	101.0	-93	-10	-13	-10	1.78	-
KIV	115.0	115.0	-40	-5	-10	-13	4.3	-
KMV+KIC	129.5	129.5	-40	-5	-10	-13	7.3	-
ITA	129.0	85.0	-50	-4	-13	-8	5.0	-

Crystallization and structure determination. Screening for crystallization was performed with hBCAT2 in 96-well sitting-drop plates, mixing 200 nL protein solution with 200 nL

precipitant solution. Commercially available screens as well as in-house were used. An initial hit was found in the MemGold2 (Molecular Dimensions) consisting of 0.01 M Zinc acetate dihydrate, 1.5 M Ammonium sulfate, 0.1 M MES, pH 6.0. This condition was further optimized through different concentrations of Ammonium sulfate, Zinc acetate dihydrate and pH values, which produced the final crystallization condition: 0.01 M Zinc acetate dihydrate, 1.5 M Ammonium sulfate, 0.1 M MES, pH 6.0.

For crystallization of hBCAT2 in complex with itaconate, hBCAT2 (10 mg/mL) and itaconate mixture was then mixed in a 1:150 ratio. The mixture was incubated at 4°C for 1 hour. The sitting-drop vapor diffusion method was performed by mixing 1 μL protein sample and 1 μL crystallization solution [0.01 M Zinc acetate dihydrate, 1.5 M Ammonium sulfate, 0.1 M MES, pH 6.0] to give a final drop size of 2 μl. The hBCAT2-itaconate crystals were grown at 18°C. After 1-7 days, triangular-shaped crystals appeared. Crystals were cryoprotected in crystallization solution modified to include 30 % glycerol before frozen in liquid nitrogen.

The hBCAT2 structure determination followed the protocol described by our previously reported paper. The X-ray diffraction data were collected at Shanghai Synchrotron Radiation Facility (SSRF) beamline BL18U1. The diffraction data were indexed, integrated, and scaled using HKL2000 (HKL Research). The structure was determined by molecular replacement using the published hBCAT2 structure (PDB ID:1EKF)[2] as the search model using the Phaser program[3]. The structural model was then adjusted in Coot[4] and refined using Phenix. The quality of the structural model was checked using the MolProbity program in Phenix [5]. The crystallographic data and refinement statistics are summarized

Statistical analysis. Results are shown as mean ± s.d. Fold change in relation to control groups of three independent cell culture and subsequent procedures. Student's t-test was used to compare experimental data. We analyzed the data in GraphPad Prism (GraphPad Software 9.4.0), using the unpaired, two-tailed t-test module. Statistical significance was considered when a p value was below 0.05. *p< 0.05; **p < 0.01; ***p < 0.001; ****p < 0.0001. N.S. not significant.

Supplementary Table S1.

ITA-interacting targets as identified by TPP.

TPP-identified ITA targets with the ΔTm values exceeding 1°C in all three biological replicates and a relatively significant P value. (n = 190)

Uniprot Accession	Gene name	ΔTm(ITA-PBS)				Captured by ITalk?
		Rep.1	Rep.2	Rep.3	Average	
Q62351	Tfrc	2.1	1.3	10.8	4.7	
Q8R1F9	Rpp40	7.0	2.2	3.8	4.3	
Q922Q8	Lrrc59	1.0	4.5	5.3	3.6	
Q14B71	Cdca2	2.3	1.0	7.1	3.5	
Q64012	Raly	3.1	4.1	2.5	3.2	
Q3TWW8	Srsf6	4.6	1.5	3.6	3.2	
P10922	H1-0	3.2	1.9	4.5	3.2	
Q8K4P0	Wdr33	2.8	1.1	2.0	2.0	Yes
P70460	Vasp	1.9	2.7	2.6	2.4	Yes
Q9CQL7	Mrfap1	3.3	2.7	2.9	3.0	
Q60809	Cnot7	2.6	2.7	3.4	2.9	
Q9D404	Oxsm	3.8	1.5	3.3	2.9	
Q9Z0P5	Twf2	1.1	1.1	1.9	1.4	Yes
P09405	Ncl	3.7	2.0	2.5	2.8	
Q60838	Dvl2	1.1	1.7	5.5	2.7	
Q9QZB9	Dctn5	4.8	2.2	1.1	2.7	
Q9D853	Eef1akmt2	3.5	2.4	2.1	2.7	
Q61194	Pik3c2a	2.7	1.1	4.2	2.7	
Q8K215	Lyrm4	2.2	4.4	1.2	2.6	
Q91YD3	Dcp1a	2.2	3.3	2.2	2.6	
P43274	H1-4	2.9	2.1	2.8	2.6	
Q62276	Med22	3.7	2.2	1.9	2.6	
Q7TSE6	Stk38l	1.2	1.7	4.8	2.6	
Q3UMT1	Ppp1r12c	3.4	1.5	2.7	2.6	
P63330	Ppp2ca	2.6	1.2	3.9	2.6	
O54781	Srpk2	2.8	1.7	3.1	2.5	
Q9QZS3	Numb	2.9	1.0	3.7	2.5	
Q9CYF5	Rcc1l	2.1	3.4	2.0	2.5	
Q3TXU5	Dhps	1.6	1.8	4.1	2.5	
Q9Z0H8	Clip2	2.8	1.0	3.6	2.5	
Q9QZR0	Rnf25	3.3	1.2	2.8	2.4	
Q4VBE8	Wdr18	2.6	1.8	3.0	2.4	
Q9Z204	Hnrnpc	2.7	2.2	2.3	2.4	
Q61033	Tmpo	2.0	1.4	2.1	1.8	Yes

Uniprot Accession	Gene name	ΔTm(ITA-PBS)				Captured by ITalk?
		Rep.1	Rep.2	Rep.3	Average	
P46737	Brcc3	1.1	2.3	3.7	2.4	
Q497K7	Tmem247	3.8	1.0	2.3	2.4	
Q99J99	Mpst	2.4	1.4	3.3	2.4	
Q9CQA3	Sdhb	3.6	2.1	1.4	2.4	
A3KGF7	Plcb2	1.6	1.4	4.1	2.4	
Q9CWS4	Ints11	1.7	1.1	4.3	2.3	
E9PYK3	Parp4	1.5	1.3	4.0	2.3	
Q04692	Smarcad1	1.7	1.4	1.9	1.6	Yes
Q8K3W0	Babam2	1.2	2.1	3.5	2.3	
P42208	Septin2	2.1	2.0	2.3	2.1	Yes
Q60739	Bag1	3.2	1.4	2.1	2.2	
P17742	Ppia	1.8	1.8	3.1	2.2	
Q99KX1	Mlf2	2.8	1.9	1.9	2.2	
Q80WT5	Aftph	2.7	1.6	2.3	2.2	
O70492	Snx3	1.3	2.9	2.4	2.2	
Q920B9	Supt16h	1.6	1.2	3.8	2.2	
O89017	Lgmn	2.6	2.1	1.8	2.2	
Q9CWW7	Cxxc1	1.6	1.9	3.0	2.2	
Q8K2B3	Sdha	2.4	1.4	2.6	2.2	
Q7TMY4	Thoc7	1.8	1.4	3.3	2.1	
Q8BIJ7	Rufy1	1.6	1.0	1.9	1.5	Yes
P47964	Rpl36	2.1	1.7	2.6	2.1	
P12970	Rpl7a	2.1	1.2	3.0	2.1	
O35855	Bcat2	3.0	1.1	2.1	2.1	
Q8BKT7	Thoc5	1.7	1.2	3.3	2.1	
Q8BJW6	Eif2a	1.2	1.3	3.7	2.1	
Q8K284	Gtf3c1	2.0	1.4	2.8	2.0	
Q8BVY0	Rsl1d1	1.9	1.4	1.4	1.5	Yes
Q8BWT1	Acaa2	2.6	1.3	2.2	2.0	
Q9D0W5	Ppil1	1.8	1.8	2.5	2.0	
Q6PIU9	Q6PIU9	1.4	1.1	3.6	2.0	
O88487	Dync1i2	3.1	1.9	1.1	2.0	
P62852	Rps25	1.4	1.1	1.3	1.2	Yes
Q9DCE5	Pak1ip1	1.6	1.0	3.3	2.0	
Q8CF89	Tab1	1.7	2.3	1.9	2.0	
B2RY56	Rbm25	2.2	1.2	1.9	1.7	Yes
Q5ND34	Wdr81	1.4	1.3	3.2	2.0	
Q9CRA5	Golph3	2.9	1.7	1.3	2.0	
P12367	Prkar2a	1.5	1.6	1.5	1.6	Yes
Q8BW10	Nob1	3.0	1.5	1.3	1.9	
P50136	Bckdha	1.1	2.4	2.4	1.9	

Uniprot Accession	Gene name	ΔTm(ITA-PBS)				Captured by ITalk?
		Rep.1	Rep.2	Rep.3	Average	
Q7JJ13	Brd2	3.1	1.1	1.6	1.9	
Q8R001	Mapre2	1.2	1.5	3.1	1.9	
Q8C167	Prepl	1.7	1.1	3.0	1.9	
P97287	Mcl1	1.6	2.7	1.4	1.9	
Q8C854	Myef2	2.5	2.1	1.2	1.9	
Q99M04	Lias	1.1	1.8	2.8	1.9	
Q8VDM1	Zgpat	2.2	1.7	1.8	1.9	
P35700	Prdx1	1.2	1.4	3.4	2.0	Yes
Q9CR70	Lage3	1.7	1.9	2.0	1.9	
Q70FJ1	Akap9	2.1	1.2	2.2	1.8	
Q61074	Ppm1g	1.8	1.5	2.8	2.0	Yes
Q08024	Cbfb	2.2	2.2	1.1	1.8	
Q9R060	Nubp1	1.4	1.9	2.3	1.9	Yes
Q9WTK5	Nfkb2	1.1	1.2	1.2	1.2	Yes
Q60605	Myl6	1.4	1.3	2.8	1.8	
P33215	Nedd1	3.3	1.1	4.2	2.9	Yes
P63276	Rps17	3.0	1.3	1.2	1.8	
P18242	Ctsd	1.1	1.6	2.7	1.8	
Q8BTS4	Nup54	1.5	2.2	1.7	1.8	
Q80UK7	Sass6	2.3	1.2	2.0	1.8	
Q9JIK5	Ddx21	2.7	1.2	1.5	1.8	
P81069	Gabpb2	1.3	1.2	2.8	1.8	
Q9JJA2	Cog8	1.3	3.0	1.0	1.8	
Q99JX3	Gorasp2	1.1	1.4	2.8	1.8	
Q9DCS3	Mecr	1.7	2.0	1.6	1.7	
Q6PEB6	Mob4	2.0	1.5	2.0	1.8	Yes
Q91YN9	Bag2	2.0	1.8	1.3	1.7	
P36552	Cpox	2.6	1.3	1.3	1.7	
Q9DCN1	Nudt12	2.6	1.4	1.1	1.7	
P08207	S100a10	2.5	1.0	1.6	1.7	
Q99LM2	Cdk5rap3	1.7	1.0	2.3	1.7	
Q8BG30	Nelfa	3.0	1.1	1.0	1.7	
Q9ERD8	Parvg	1.6	1.4	2.0	1.7	
O09131	Gsto1	1.5	1.0	2.4	1.7	
Q9D483	Polr3c	1.9	1.2	1.9	1.7	
Q9CV28	Mindy3	2.3	1.7	2.8	2.3	Yes
Q9D0E1	Hnrnpm	2.0	1.1	1.8	1.6	Yes
Q8R395	Commd5	1.8	1.6	1.4	1.6	
Q9Z2X1	Hnrnpf	1.4	2.5	1.5	1.8	Yes
Q99KR7	Ppif	2.1	1.1	1.7	1.6	
O55125	Nipsnap1	1.4	2.2	1.3	1.6	

Uniprot Accession	Gene name	ΔTm(ITA-PBS)				Captured by ITalk?
		Rep.1	Rep.2	Rep.3	Average	
Q8CFI2	Cdc34	1.9	1.8	1.2	1.6	
Q8QZT1	Acat1	1.3	1.6	2.0	1.6	
G5E897	Poglut3	1.8	1.2	1.8	1.6	
Q9DCJ1	Mlst8	1.0	1.4	2.4	1.6	
Q80UK8	Ints2	1.9	1.2	1.7	1.6	
P50295	Nat2	1.1	1.4	2.3	1.6	
B1AVY7	Kif16b	1.6	1.3	1.9	1.6	
Q9JJI8	Rpl38	2.0	1.3	1.5	1.6	
P59470	Polr3b	1.4	1.1	2.2	1.6	
B1AZI6	Thoc2	1.9	1.7	1.1	1.6	
Q6PGF7	Exoc8	1.5	1.4	1.9	1.6	
Q91YP2	Nln	1.3	1.6	1.8	1.6	
O08915	Aip	1.7	1.5	1.5	1.6	
P47963	Rpl13	1.6	1.4	1.6	1.6	
P38060	Hmgcl	1.5	1.7	1.3	1.5	Yes
P14733	Lmnb1	1.5	1.2	1.9	1.6	
Q9Z2V5	Hdac6	1.6	1.0	1.3	1.3	Yes
Q9ERF3	Skic8	1.6	1.1	1.9	1.5	
A2AGH6	Med12	1.8	1.3	1.5	1.5	
Q8CI11	Gnl3	1.5	1.1	2.3	1.7	Yes
Q6P5E6	Gga2	1.2	2.1	1.3	1.5	
Q08509	Eps8	1.8	1.2	1.6	1.5	
Q99LB6	Mat2b	1.3	1.2	2.1	1.5	
P62137	Ppp1ca	1.6	1.1	1.9	1.5	
Q3UQN2	Fcho2	1.2	1.2	2.2	1.5	
Q6NZJ6	Eif4g1	1.1	1.0	1.6	1.2	Yes
P46718	Pdcd2	2.2	1.1	1.2	1.5	
P56546	Ctbp2	1.3	1.1	2.0	1.5	
Q8CI75	Dis3l2	1.7	1.1	1.6	1.5	
Q8K297	Colgalt1	1.6	1.5	1.3	1.5	
Q7TMK6	Hook2	1.3	1.8	1.3	1.5	
Q9JHI5	Ivd	1.0	1.6	1.8	1.5	
Q6P1E1	Zmiz1	1.2	1.3	2.0	1.5	
Q9EPU4	Cpsf1	1.9	1.1	1.4	1.5	
Q9Z1E4	Gys1	1.8	1.5	1.0	1.5	
Q8C147	Dock8	1.2	1.0	1.0	1.1	Yes
Q9EST5	Anp32b	1.5	1.4	1.4	1.4	
Q9Z0H3	Smarcb1	1.1	1.1	2.1	1.4	
Q9D868	Ppih	1.9	1.1	1.3	1.4	
Q9WTP7	Ak3	1.7	1.1	1.4	1.4	
Q6P7W5	Tsen2	1.5	1.3	1.4	1.4	

Uniprot Accession	Gene name	ΔTm(ITA-PBS)				Captured by ITalk?
		Rep.1	Rep.2	Rep.3	Average	
Q9WUD1	Stub1	1.1	1.2	1.8	1.4	
P47911	Rpl6	1.5	1.6	1.1	1.4	
P62242	Rps8	1.3	1.6	1.2	1.4	
Q80VJ3	Dnph1	1.7	1.3	2.8	2.0	Yes
Q3U308	Ctu2	1.5	1.3	1.2	1.4	Yes
Q8K4M5	Commd1	1.6	1.2	1.4	1.4	
O08539	Bin1	1.2	1.0	1.9	1.4	
Q5FWK3	Arhgap1	1.5	1.3	1.3	1.4	
Q99J10	Ctu1	1.9	2.2	1.5	1.8	Yes
P0DOV2	Ifi204	1.3	1.6	1.0	1.3	
Q61187	Tsg101	1.2	1.8	1.1	1.3	
A2AGT5	Ckap5	1.6	1.4	1.4	1.4	Yes
Q8BW96	Camk1d	2.0	1.4	3.3	2.2	Yes
Q9CY94	Gins3	1.6	1.3	1.1	1.3	
Q8K298	Anln	1.1	1.4	1.4	1.3	
Q923E4	Sirt1	1.4	1.2	1.3	1.3	
P62754	Rps6	1.2	1.4	1.2	1.3	
Q9D6R2	Idh3a	1.1	1.0	1.7	1.3	
Q91YS8	Camk1	1.3	1.1	1.2	1.2	Yes
A2APY7	Ndufaf5	1.0	1.1	1.6	1.2	
Q8R0X2	Cacul1	1.7	2.2	5.2	3.0	Yes
B1AVH7	Tbc1d2	1.2	1.2	1.3	1.2	
Q99LC5	Etfa	1.1	1.0	1.5	1.2	
Q8VCT3	Rnpep	1.1	1.2	1.3	1.2	
Q8K012	Fnbp1l	1.0	1.2	1.4	1.2	
P53762	Arnt	1.2	1.2	1.6	1.3	Yes
Q921X9	Pdia5	1.2	1.1	1.3	1.2	
Q8CJG0	Ago2	5.4	1.7	2.3	3.1	Yes
Q8K354	Cbr3	1.3	1.1	1.0	1.2	
P28271	Aco1	1.2	1.1	1.1	1.2	
Q5DTM8	Rnf20	1.0	1.1	1.4	1.2	
Q80XQ2	Tbc1d5	1.3	1.0	1.1	1.1	
Q921H8	Acaa1a	1.2	1.2	1.8	1.4	Yes

Supplementary Table S2.

Crystallographic data collection and refinement statistics for the hBCAT2-ITA complex.

	hBCAT2-ITA
Data collection	
Space group	*P*32
Cell dimensions (Å)	85.582, 85.582, 106.837
α, β, γ (°)	90, 90, 120
Wavelength (Å)	0.9794
Resolution (Å)	39.72-2.0 (2.072-2.0)
CC1/2	0.990 (0.872)
Rpim	0.049 (0.259)
R_{merge}	0.144 (0.774)
I / σI	15.79 (3.14)
Completeness (%)	99.51 (96.05)
Multiplicity	9.4 (9.6)
Wilson B-factor	23.42
Refinement	
No. reflections	58835 (5689)
R_{work} / R_{free}	0.174 / 0.214
No. of atoms	
Protein	5820
Ligand/ion	48
Water	597
B-factors	
Macromolecules	26.47
Ligand/ion	25.32
Water	34.49
R.m.s deviations	
Bond lengths (Å)	0.011
Bond angles (°)	1.10
Ramachandran	
Favored (%)	97.25
Outliers (%)	0.28

Each dataset was collected from a single crystal. Values in parentheses are for highest-resolution shell.

References

1. X. Zeng, T. Wei, X. Wang, Y. Liu, Z. Tan, Y. Zhang, T. Feng, Y. Cheng, F. Wang, B. Ma, W. Qin, C. Gao, J. Xiao and C. Wang, Discovery of metal-binding proteins by thermal proteome profiling, *Nat. Chem. Biol.*, 2024, **20**, 770-778.
2. N. Yennawar, J. Dunbar, M. Conway, S. Hutson and G. Farber, The structure of human mitochondrial branched-chain aminotransferase, *Acta Crystallogr. D Biol. Crystallogr.*, 2001, **57**, 506-515.
3. A. J. McCoy, R. W. Grosse-Kunstleve, P. D. Adams, M. D. Winn, L. C. Storoni and R. J. Read, Phaser crystallographic software, *J. Appl. Crystallogr.*, 2007, **40**, 658-674.
4. P. D. Adams, P. V. Afonine, G. Bunkóczi, V. B. Chen, I. W. Davis, N. Echols, J. J. Headd, L. W. Hung, G. J. Kapral, R. W. Grosse-Kunstleve, A. J. McCoy, N. W. Moriarty, R. Oeffner, R. J. Read, D. C. Richardson, J. S. Richardson, T. C. Terwilliger and P. H. Zwart, PHENIX: a comprehensive Python-based system for macromolecular structure solution, *Acta Crystallogr. D Biol. Crystallogr.*, 2010, **66**, 213-221.
5. P. Emsley, B. Lohkamp, W. G. Scott and K. Cowtan, Features and development of Coot, *Acta Crystallogr. D Biol. Crystallogr.*, 2010, **66**, 486-501.